

# Design and Analysis of a Multi-Carrier Differential Chaos Shift Keying Communication System

Georges Kaddoum\*, François-Dominique Richardson, François Gagnon

**Abstract**—A new Multi-Carrier Differential Chaos Shift Keying (MC-DCSK) modulation is presented in this paper. The system endeavors to provide a good trade-off between robustness, energy efficiency and high data rate, while still being simple compared to conventional multi-carrier spread spectrum systems. This system can be seen as a parallel extension of the DCSK modulation where one chaotic reference sequence is transmitted over a predefined subcarrier frequency. Multiple modulated data streams are transmitted over the remaining subcarriers. This transmitter structure increases the spectral efficiency of the conventional DCSK system and uses less energy. The receiver design makes this system easy to implement where no radio frequency (RF) delay circuit is needed to demodulate received data. Various system design parameters are discussed throughout the paper, including the number of subcarriers, the spreading factor, and the transmitted energy. Once the design is explained, the bit error rate performance of the MC-DCSK system is computed and compared to the conventional DCSK system under an additive white Gaussian noise (AWGN) and Rayleigh channels. Simulation results confirm the advantages of this new hybrid design.

**Index Terms**—Chaos based communication system, Non-coherent receiver, Multi-carrier DCSK, Energy efficiency, Performance analysis.

## I. INTRODUCTION

AS computing devices become ubiquitous, a plurality of challenges emerge from the various communications paradigms. Some researchers have envisioned that there will be “Seven Trillion Wireless Devices Serving Seven Billion People by 2020” [1]. In this perspective, spectral and power efficiency, interference resistance, security and channel agnosticism are, and will continue, to be top requirements for wireless communication systems.

Mobile wireless communications performances are deteriorated by device hardware and the propagation environments [2]. Fading channels, for instance in Vehicle-to-Vehicle communication where moving scatterers cause a non-wide-sense stationary uncorrelated scattering (WSSUS) behavior [3], are typically harsh environments for mobile communications. In order to get optimal communication systems in varying channels, many techniques can be employed. One is the use of multi-carrier systems, such as OFDM, that have a high resilience to selective channels if the bandwidth of

each subcarrier is smaller than the coherence bandwidth; non-coherent communication systems make up the other. It has been stated that non-coherent systems can outperform coherent ones in fast frequency and time-varying channels, mainly because of the spectral inefficiency inherent to the insertion of pilots [4].

Several combinations of multi-carrier transmission and Code Division Multiple Access (CDMA), like Multi-Carrier CDMA (MC-CDMA), Multi-Carrier Direct-Sequence CDMA (MC-DS-CDMA) and Orthogonal Frequency Code Division Multiplexing (OFCDM) are proposed in the literature [5], [6], [7]. In MC-CDMA, one-bit chips are spread over  $M$  subcarriers in the frequency domain [5], while for MC-DS-CDMA, time and frequency spreading is used (*i.e.* TF-domain spreading) [7]. Time-domain spreading is employed to increase the processing gain in each subcarrier signal, while frequency domain spreading is used to increase the total processing gain.

The chaotic signal has a sensitive dependence upon initial conditions property that allows the generation of a theoretical infinite number of uncorrelated signals. Those signals have been shown to be well suited for spread-spectrum modulation because of their inherent wideband characteristic [8] [9] [10]. Chaotic modulations thus have similar advantages as other spread-spectrum modulations, *exempli gratia*, including the mitigation of fading channels and jamming resistance. The low probability of intercept (LPI) performance chaotic signals [11] agrees with military scenarios and in densely populated environments [12]. In addition, chaos-based sequences give good results as compared to Gold and independent and identically distributed sequences for reducing the peak-to-average power ratio (PAPR) [13].

A proposed system with a non-coherent receiver, named a differential chaos shift keying (DCSK) system, in which chaotic synchronization is not used on the receiver side, delivers a good performance in multipath channels [14] [15]. Furthermore, differential non-coherent systems are better suited than coherent ones for time and frequency selective channels [4]. In the DCSK system, each bit duration is divided into two equal slots. In the first slot, a reference chaotic signal is sent. Depending on the bit being sent, the reference signal is either repeated or multiplied by the factor  $-1$  and transmitted in the second slot. A significant drawback of DCSK is that half the bit duration is spent sending non-information-bearing reference samples [8]. This can be accounted as being energy-inefficient and a serious data rate reducer. The analytical performance derivation of DCSK communication system is studied in [16] for fading channels and in [17] [18] [19] [20] for cooperative schemes. The transmission security of DCSK

G. Kaddoum, F.-D. Richardson and F. Gagnon are with University of Québec, ETS, LaCIME Laboratory, 1100 Notre-Dame west, H3C 1K3, Montreal, Canada (e-mail: georges.kaddoum@lacime.etsmtl.ca; francois.richardson@lacime.etsmtl.ca; francois.gagnon@etsmtl.ca)

\* This work has been supported in part by Ultra Electronics TCS and the Natural Science and Engineering Council of Canada as part of the ‘High Performance Emergency and Tactical Wireless Communication Chair’ at École de technologie supérieure.

system is improved in [21]. In [22], the spectral efficiency of the DCSK is improved, but the system receiver requires an RF delay line, which is not easy to implement because of the wide bandwidth involved. In a study to overcome the problem of RF delay in DCSK systems, Xu *et al.* proposed a Code Shifted Differential Chaos Shift Keying (CS-DCSK) system [23]. In their system, the reference and the information bearing signals are separated by Walsh code sequences, and then transmitted in the same time slot. For such systems, there is no need for a delay line at the receiver end. An improved version of the high spectral efficiency DCSK system by [23] is presented in [24], where chaotic codes are used instead of Walsh codes, with different receiver structures. Because of these advantages, some ultrawideband systems based on DCSK or FM-DCSK modulations have been proposed for wireless personal area networks [25], [26], [27].

In this paper, we first introduce a new design of a multi-carrier DCSK system (MC-DCSK). The system is a hybrid of multi-carrier and DCSK modulations. On the transmitter side, one of the  $M$  subcarriers is assigned to transmitting the reference slot, while the other frequencies will carry the data slots. In this case, just one chaotic reference is used to transmit  $M - 1$  bits, which saves the transmitted bit energy and the data rate. After the subcarriers are removed, a parallel demodulation is achieved to quickly recover the transmitted bits. The proposed system solves the RF delay line problem mentioned in [23], provides from the properties of DCSK system in terms of resistance to interference, increases the data rate, and optimizes the transmitted energy of the DCSK system with a simple transmitter/receiver design compared to conventional multi-carrier spread spectrum systems (i.e MC-DS-CDMA).

Secondly, we thoroughly analyze the performance under AWGN and Rayleigh fading channel, without neglecting the dynamic properties of chaotic sequences, meaning that in our computation approach, the transmitted bit energy is not considered as constant. Many approaches have been considered for computing the bit error rate performances of the DCSK system, such as Gaussian approximation (GA). This approximation assumes that the correlator output follows the normal distribution. Applied to the DCSK system over an AWGN or multipath channel in [28], this method provides rather good estimates of the BER for very large spreading factors, but when the spreading factor is small, the results produced by the Gaussian approximation method are rather disappointing. Another accurate computation methodology is developed in [29],[30] and [31] to compute the BER performance DCSK over different wireless channels. Their approach enables the dynamics properties of the chaotic sequence by integrating the BER expression for a given chaotic map over all possible chaotic sequences for a given spreading factor. This latter method is compared to the BER computation under the Gaussian assumption in [31], and seems more realistic to match the exact BER. However, as indicated in [31], [30], the drawback of the proposed method is the high calculation difficulty. Since approaches that have been previously presented so far are either invalid for small spreading factors or involving highly complex computations, we extend a simple

and accurate method in this paper for computing the exact performance for a single-user MC-DCSK system. The system is evaluated first over an AWGN to highlight the problem of non constant bit energy. Then, the performance of MC-DCSK system is evaluated under Rayleigh fading channel. The proposed method includes the computation of the probability density function of the chaotic bit energy and the integration of the BER over all possible values of the PDF. The advantage of this method lies in the fact that it gives an exact BER expression without neglecting the dynamical properties of chaotic sequences with low computing charges.

Thirdly, we derive the analytical bit error rate expressions, and we show the accuracy of our analysis by matching the exact numerical performance, especially when the spreading factor is low. We can conclude that the proposed system can be suited for Wireless Sensor Network (WSN) applications [32], which are power-limited and evolve in harsh environments.

The remainder of this paper is organized as follows. In section II, the characteristics of chaos-based systems are described with an emphasis on DCSK. The III section covers the architecture of the MC-DCSK system. The energy and spectral efficiencies of the system are examined in section IV. The performance analysis is explained in section V. Simulation results and discussions are presented in section VI, and concluding remarks are presented in section VII.

## II. DCSK COMMUNICATION SYSTEM AND WEAKNESS POINTS

In this section, the DCSK communication system, together with its weakness points, are discussed. The conventional DCSK modulation scheme will be used in section VI as a comparative to illustrate the performance enhancements obtained from the main contribution of this paper.

### A. DCSK communication system

As shown in Figure 1, within the modulator, each bit  $s_i = \{-1, +1\}$  is represented by two sets of chaotic signal samples, with the first set representing the reference, and the second carrying data. If  $+1$  is transmitted, the data-bearing sequence is equal to the reference sequence, and if  $-1$  is transmitted, an inverted version of the reference sequence is used as the data-bearing sequence. Let  $2\beta$  be the spreading factor in DCSK system, defined as the number of chaotic samples sent for each bit, where  $\beta$  is an integer. During the  $i^{th}$  bit duration, the output of the transmitter  $e_{i,k}$  is

$$e_{i,k} = \begin{cases} x_{i,k} & \text{for } 1 < k \leq \beta, \\ s_i x_{i,k-\beta} & \text{for } \beta < k \leq 2\beta, \end{cases} \quad (1)$$

where  $x_k$  is the chaotic sequence used as reference and  $x_{k-\beta}$  is the delayed version of the reference sequence.

Figure 1 illustrates that the received signal  $r_k$  is correlated to a delayed version of the received signal  $r_{k+\beta}$  and summed over a bit duration  $T_b$  (where  $T_b = \beta T_c$  and  $T_c$  is the chip time) to demodulate the transmitted bits. The received bits are estimated by computing the sign of the output of the correlator (i.e., see Figure 1 (c) the DCSK receiver).

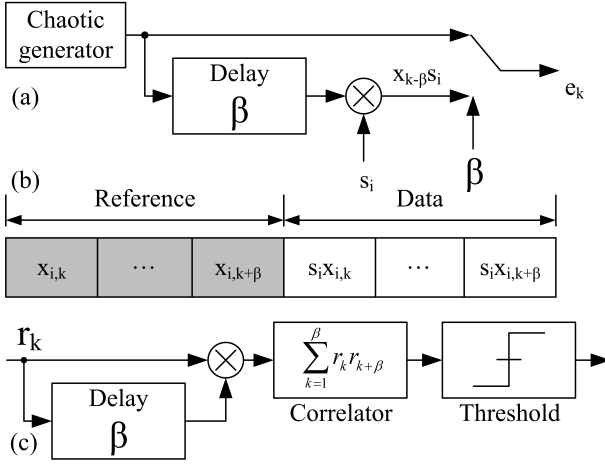


Fig. 1. Block diagram of the general structure of the DCSK communication system. (a) is the DCSK transmitter, (b) represents the DCSK frame (c) is the DCSK receiver.

### B. Weakness of DCSK

In this paper, we are not working on improving the inherent lack of security of non-coherent systems, as the security issue was addressed in our previous work [21], where a secure chaos-based multi-carrier communication system was proposed. Our focus in this work is on the spectral and energy efficiencies having a good performance.

As shown in Figure 1, half the bit duration time is spent sending a non-information-bearing reference. Therefore, the data rate of this architecture is seriously reduced compared to other systems using the same bandwidth, leading to a loss of energy. The reference sequence dissipates half the energy of each bit.

## III. MULTI-CARRIER DCSK SYSTEM ARCHITECTURE

The system's architecture is intended to be of low complexity. Numerous extensions could be performed to this system for different performance optimizations. The system presented here is in its most elementary form.

### A. Chaotic generator

In this paper, a second-order Chebyshev polynomial function (CPF) is employed

$$x_{k+1} = 1 - 2x_k^2. \quad (2)$$

This map is chosen for the ease with which it generates chaotic sequences and the good performance [33]. In addition, chaotic sequences are normalized such that their mean values are all zero and their mean squared values are unity, i.e.,  $E(x_k) = 0$  and  $E(x_k^2) = 1$ .

### B. The transmitter

The MC-DCSK system benefits from the non-coherent advantages of DCSK and the spectral efficiency of multi-carrier modulation. In this system, the input information sequence is first converted into  $U$  parallel data sequences  $s_u(t)$  for

$u = 1, 2, \dots, U$ . The independent data sequence  $s_u(t)$  with equal probability value is  $+1$ , or  $-1$ , where

$$s_u(t) = \sum_{i=1}^{M-1} s_{u,i}(t). \quad (3)$$

where  $s_{u,i}$  is the  $i^{th}$  bit of the  $u^{th}$  sequence data and  $M-1$  is the number of data per  $u^{th}$  sequence.

As shown in Figure 2, a reference chaotic code  $x_u(t)$  to be used as a reference signal and spreading code. After a serial-to-parallel conversion, the  $M-1$  bits stream of the  $u^{th}$  data sequence are spread due to multiplication in time with the same chaotic spreading code  $x_u(t)$ .

$$x_u(t) = \sum_{k=1}^{\beta} x_{u,k} h(t - kT_c), \quad (4)$$

where,  $\beta$  is the spreading factor,  $h(t)$  is the square-root-raised-cosine filter. This filter is band-limited and is normalized to have unit energy. Let  $H(f) = F\{h(t)\}$ , where  $F$  denotes a Fourier transform. It is assumed that  $H(f)$  is limited to  $[-B_c/2, B_c/2]$  which satisfies the Nyquist criterion with a rolloff factor  $\alpha$  ( $0 \leq \alpha \leq 1$ ) where  $B_c = (1 + \alpha)/T_c$ .

The chaotic signal  $x_u(t)$  modulates the first subcarrier as reference, after which the data signals spread by  $M-1$  modulate the  $M-1$  subcarriers.

Therefore, the transmitted signal of the MC-DCSK is given by:

$$e(t) = x_u(t) \cos(2\pi f_1 t + \phi_1) + \sum_{i=2}^M s_{u,i}(t) x_u(t) \cos(2\pi f_i t + \phi_i), \quad (5)$$

where  $\phi_i$  represents the phase angle introduced in the carrier modulation process. In this paper, we normalize the transmitted energy in every subcarrier.

For the MC-DCSK, the modulated subcarriers are orthogonal over the chip duration. Hence, the baseband frequency corresponding to the  $i^{th}$  subcarrier is  $f_i = f_p + i/T_c$ , where  $f_p$  is the fundamental subcarrier frequency. The minimum spacing between two adjacent subcarriers equals  $\Delta = (1 + \alpha)/T_c$ , which is a widely used assumption [7].

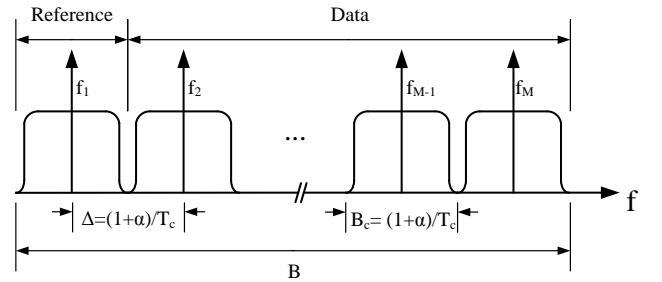


Fig. 3. The power spectral density of a band-limited MC-DCSK system.

Figure 3 shows the power spectral density (PSD) of the MC-DCSK system. Let  $B$  be the total bandwidth of the proposed system. When both bit duration  $T_b$  and  $B$  are set, the chip duration  $T_c$  as well as the spreading factor  $\beta$  depend on the

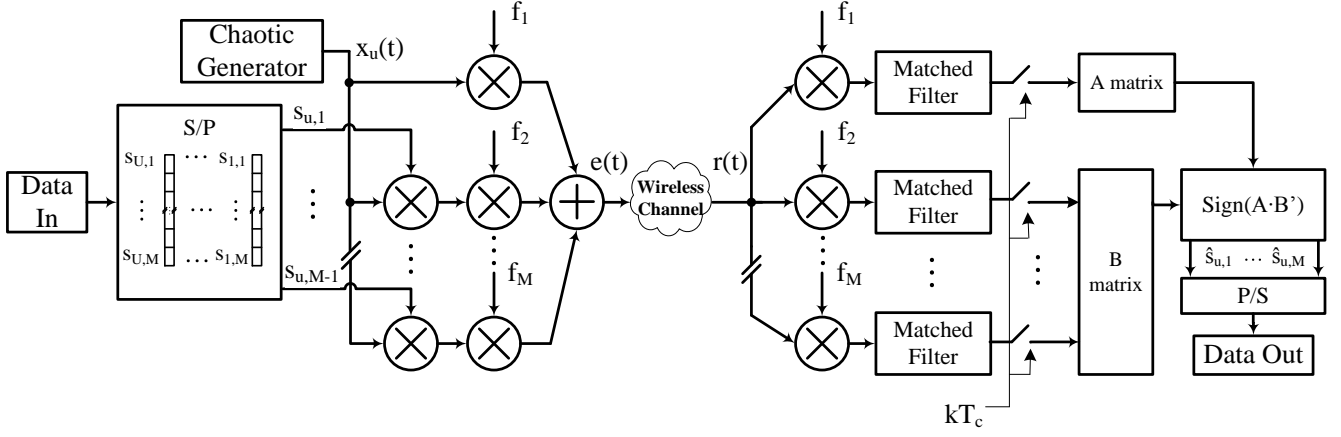


Fig. 2. Block diagram of the MC-DCSK system

number of subcarrier  $M$ , the bandwidth  $B_c$  of each subchannel or the subcarrier spacing  $\Delta$ . In our design, we divide the total band  $B$  into  $M$  equi-width frequency bands, as shown in Figure 3, where all bands are disjoint. The bandwidth of each subcarrier band  $B_c$  is:

$$B_c = (1 + \alpha)/T_c.$$

The total required bandwidth  $B$  is:

$$B = MB_c,$$

$$B = M(1 + \alpha)/T_c.$$

Thus, the spreading factor function of the system parameters is:

$$\beta = T_b/T_c, \quad (6)$$

$$\beta = \frac{T_b B}{M(1 + \alpha)}.$$

In order to validate our system design and evaluate its parameters, such as the spreading factor, the bit energy, the bit error rate performance, and the spectral efficiency. The received signal is:

$$r(t) = \lambda(t)e(t) + n(t), \quad (7)$$

where  $\lambda(t)$  is the channel coefficient,  $n(t)$  is an wideband AWGN with zero mean and power spectral density of  $N_0/2$ .

In our paper,  $\lambda(t) = 1$  for AWGN case. Otherwise, for fading channel analysis, has a Rayleigh probability density function given by :

$$f_\lambda(z) = \frac{z}{\sigma^2} e^{-\frac{z^2}{2\sigma^2}} \quad z > 0. \quad (8)$$

In our paper, the channel coefficients are assumed to be constant during a frame of MC-DCSK symbols and change to new independent values from one frame to another.

### C. The receiver

The block diagram of the MC-DCSK receiver is illustrated in Figure 2. One of the objectives of this design was to provide a robust receiver providing good performance. We consider a set of matched filters, each demodulating the desired signal of the corresponding carrier frequency  $f_i$ , and then the signals are sampled every  $kT_c$  time. The outputs discrete signals are stored in matrix memory. The matrix implementation of the receiver simplifies the parallel data recovery, where the decoding algorithm is described as follow under AWGN channel:

First, at the same time, the output of the first match is stored in matrix  $P$  and the  $M - 1$  data signals are stored in the second matrix  $S$ , where:

$$P = (x_{u,1} + n_{u,1}, x_{u,2} + n_{u,2}, \dots, x_{u,\beta} + n_{u,\beta}),$$

where  $n_{u,k}$  is the  $k^{th}$  sample of additive Gaussian noise added to the reference signal.

The matrix  $S$  is:

$$S = \begin{pmatrix} s_{u,1}x_{u,1} + n_{u,1}^1 & \dots & s_{u,1}x_{u,\beta} + n_{u,\beta}^1 \\ \vdots & \vdots & \vdots \\ s_{u,M-1}x_{u,1} + n_{u,1}^{M-1} & \dots & s_{u,M-1}x_{u,\beta} + n_{u,\beta}^{M-1} \end{pmatrix}.$$

where  $n_{u,k}^i$  is the  $k^{th}$  sample of additive Gaussian noise added to the  $i^{th}$  bit of  $u^{th}$  data sequence.

Finally, after  $\beta$  clock cycles, all the samples are stored, and the decoding step is activated. The transmitted  $M - 1$  bits are recovered in parallel by computing the sign of the resultant vector of the matrix product:

$$\hat{s}_u = \text{sign}(P \times S'). \quad (9)$$

where  $\times$  is the matrix product and  $'$  is the matrix transpose operator. In fact, this matrix product can be seen as a set of a parallel correlator where the reference signal multiplies each data slot, and the result is summed over the duration  $\beta T_c$ .

#### IV. ENERGY EFFICIENCY

The energy efficiency of the proposed system is improved as compared to the DCSK system. In fact, for the DCSK system, a new chaotic reference is generated for every transmitted bit, and in our case, one reference is shared with  $M - 1$  modulated bits. For a conventional DCSK system, the transmitted bit energy  $E_b$  is:

$$E_b = E_{data} + E_{ref} \cdot \quad (10)$$

where  $E_{data}$  and  $E_{ref}$  are the energies to transmit the data and reference respectively. Without loss of generality, the data and the reference energies are equal:

$$E_{data} = E_{ref} = T_c \sum_{k=1}^{\beta} x_{i,k}^2 \cdot \quad (11)$$

Then for DCSK system, the transmitted energy  $E_b$  for a given bit  $i$  is:

$$E_b = 2T_c \sum_{k=1}^{\beta} x_{i,k}^2 \cdot \quad (12)$$

In the MC-DCSK system, one reference energy  $E_{ref}$  is shared with  $M - 1$  transmitted bit, then the energy of one given bit is the sum of its data carrier energy and a part of the reference energy:

$$E_b = E_{data} + \frac{E_{ref}}{M - 1} \cdot \quad (13)$$

In our system, the energies on the  $M$  subcarriers are equal:

$$E_{data} = E_{ref} = T_c \sum_{k=1}^{\beta} x_{i,k}^2 \cdot \quad (14)$$

The bit energy expression function of  $E_{data}$  is:

$$E_b = \frac{M}{M - 1} E_{data} \cdot \quad (15)$$

To study the energy efficiency, we compute the transmitted Data-energy-to-Bit-energy Ratio (DBR):

$$DBR = \frac{E_{data}}{E_b} \cdot \quad (16)$$

For the MC-DCSK system the DBR is:

$$DBR = \frac{M - 1}{M} \cdot \quad (17)$$

In a conventional DCSK system (i.e for  $M = 2$ ), half the energy  $E_b$  is transmitted into the reference for each bit, and then the DBR is:

$$DBR = \frac{1}{2} \cdot \quad (18)$$

As shown in Figure 4, for  $M = 2$  where we have one new reference for every bit bit, in this case, the MC-DCSK system is equivalent to a DCSK system with  $DBR = \frac{1}{2}$ . This means that 50% of the bit energy  $E_b$  is used to transmit the reference used for one bit. For the same bit energy  $E_b$ , in MC-DCSK

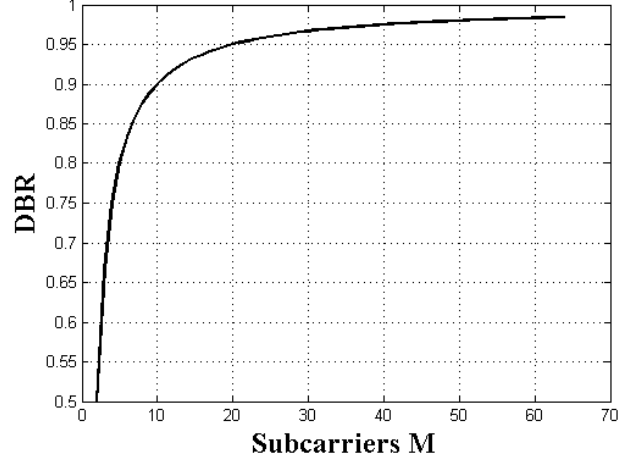


Fig. 4. DBR for a system for various amount of data subcarriers.

system, we can see for example that for  $M > 20$ , the reference energy accounts for less than 5% of the total bit energy  $E_b$  for each bit of the  $M - 1$  data stream. This mean that the energy used to transmits the reference is shared with  $M - 1$  bits.

#### V. PERFORMANCE ANALYSIS OF MC-DCSK

In this section, the performance of the MC-DCSK system is evaluated, and the analytical BER expression is derived under an AWGN and Rayleigh fading channels. To derive the analytical BER expression, the mean and the variance of the observation signal  $D_{u,i}$  must be evaluated. We start by mentioning some properties of chaotic signals which will be used later in this paper to compute the mean and the variance of the observation. The chaotic generator is very sensitive to initial conditions, and we can deduce that the different chaotic sequences generated from different initial conditions are independent from each other. In addition, the independence between the chaotic sequence and the Gaussian noise is also true [8]. For the normalized chaotic map with zero mean, the variance ( $Var(\cdot)$ ) is equal to one ( $Var(x) = E(x^2) = 1$ ).

Since the channel coefficients are assumed to be constant and the same for all frequencies during a frame of MC-DCSK symbols and change to new independent values from one frame to another. The decision variable for the  $i^{th}$  bit of the  $u^{th}$  data stream at the output of the correlator is:

$$D_{u,i} = T_c \sum_{k=1}^{\beta} (\lambda_u x_{u,k} s_{u,i} + n_{u,k}^i) (\lambda_u x_{u,k} + n_{u,k}), \quad (19)$$

where  $\lambda_u$  is the channel coefficient for the  $u^{th}$  data stream.  $n_{u,k}$  and  $n_{u,k}^i$  are two independent zero Gaussian noises coming from the reference and the  $i^{th}$  bit subcarrier.

$$D_{u,i} = T_c s_{u,i} \sum_{k=1}^{\beta} \lambda_u^2 x_{u,k}^2 + T_c \sum_{k=1}^{\beta} n_{u,k} n_{u,k}^i + T_c \sum_{k=1}^{\beta} x_{u,k} (\lambda_u n_{u,k}^i + \lambda_u s_{u,i} n_{u,k}), \quad (20)$$

where  $T_c$  is the time chip. The  $i^{th}$  bit of the  $u^{th}$  data stream is decoded by comparing the output  $D_{u,i}$  to a threshold zero. For mathematical simplification we set the time chip equal to one ( $T_c = 1$ ).

In the decision variable equation, the first term is the useful signal, while the second and third are zero-mean additive noises.

The output of the correlator for the MC-DCSK of equation (20) can be written in the form

$$D_{u,i} = s_{u,i} \frac{(M-1)\lambda_u^2 E_b^{(u)}}{M} + W + Z, \quad (21)$$

$$E_b^{(u)} = \frac{M}{M-1} T_c \sum_{k=1}^{\beta} x_{u,k}^2,$$

where  $E_b^{(u)}$  is the transmitted bit energy for a given data sequence  $u$ .

$$W = T_c \sum_{k=1}^{\beta} x_{u,k} (\lambda_u n_{u,k}^i + \lambda_u s_{u,i} n_{u,k}),$$

$$Z = T_c \sum_{k=1}^{\beta} n_{u,k} n_{u,k}^i.$$

For a given  $i^{th}$  bit of an  $u^{th}$  data stream, the instantaneous mean and variance of the decision variable are derived as follows :

$$E(D_{u,i}) = s_{u,i} \frac{(M-1)\lambda_u^2 E_b^{(u)}}{M}. \quad (22)$$

Since the three terms of (21) are uncorrelated, the noise samples and channel coefficients are independent, the conditional variance of the decision variable for a given bit  $i^{th}$  is:

$$\begin{aligned} Var(D_{u,i}) &= E \left( \left( \frac{M-1}{M} \lambda_u^2 E_b^{(u)} s_{u,i} \right)^2 \right) \\ &+ E \left( \left( \sum_{k=1}^{\beta} \lambda_u x_{u,k} n_{u,k}^i \right)^2 \right) + E \left( \left( \sum_{k=1}^{\beta} \lambda_u x_{u,k} s_{u,i} n_{u,k} \right)^2 \right) \\ &+ E \left( \left( \sum_{k=1}^{\beta} n_{u,k} n_{u,k}^i \right)^2 \right) - \left( \frac{(M-1)}{M} \lambda_u^2 E_b^{(u)} s_{u,i} \right)^2, \end{aligned} \quad (23)$$

Finally after simplification,

$$Var(D_i) = \frac{(M-1)E_b^{(u)}}{M} \lambda_u^2 N_0 / 2 + \beta N_0^2 / 4. \quad (24)$$

In order to compute the BER with our approach, the error probability must first be evaluated for a given received energy  $E_b^{(u)}$  and the channel coefficient  $\lambda_u$ . Considering the bit energy (or chaotic chips) as a deterministic variable, the decision variable at the output of the correlator is necessarily a random Gaussian variable. Using equations (22), (24), the bit error probability is :

$$\begin{aligned} BER &= \frac{1}{2} \Pr(D_{u,i} < 0 | s_{u,i} = +1) + \frac{1}{2} \Pr(D_{u,i} > 0 | s_{u,i} = -1) \\ &= \frac{1}{2} \operatorname{erfc} \left( \frac{E[D_{u,i} | s_{u,i} = +1]}{\sqrt{2 \operatorname{Var}[D_{u,i} | s_{u,i} = +1]}} \right), \end{aligned} \quad (25)$$

where  $\operatorname{erfc}(x)$  is the complementary error function defined by:

$$\operatorname{erfc}(x) \equiv \frac{2}{\sqrt{\pi}} \int_x^{\infty} e^{-\mu^2} d\mu$$

The BER expression for the MC-DCSK system is:

$$BER = \frac{1}{2} \operatorname{erfc} \left( \left[ \frac{MN_0}{(M-1)\lambda_u^2 E_b^{(u)}} + \frac{M^2 \beta N_0^2}{2(M-1)\lambda_u^4 E_b^{(u)2}} \right]^{-\frac{1}{2}} \right). \quad (26)$$

Many approaches have been considered for computing the BER of chaos-based communication systems, with the most widely used being the Gaussian approximation, which considers the transmitted bit energy  $E_b^{(u)}$  as constant [34]. Because of the non-periodic nature of chaotic signals, the transmitted bit energy after spreading by chaotic sequences definitely varies from one bit to another [35]. Based on this fact, the overall BER expression of the MC-DCSK system is then given by:

$$BER = \int_0^{+\infty} \int_0^{+\infty} \operatorname{erfc} \left( \left[ \frac{MN_0}{(M-1)\lambda^2 E_b} + \frac{M^2 \beta N_0^2}{2(M-1)\lambda^4 E_b^2} \right]^{-\frac{1}{2}} \right) f(E_b) f(\lambda) dE_b d\lambda, \quad (27)$$

where  $f(\lambda)$ , and  $p(E_b)$  are the probability density functions of channels coefficient and the bit energy  $E_b$  respectively.

The BER expression can be simplified as:

$$BER = \int_0^{+\infty} \frac{1}{2} \operatorname{erfc} \left( \left[ \frac{M}{(M-1)\gamma_b} + \frac{M^2 \beta}{2(M-1)^2 \gamma_b^2} \right]^{-\frac{1}{2}} \right) f(\gamma_b) d\gamma_b, \quad (28)$$

where  $\gamma_b = \lambda^2 E_b / N_0$  is product of two random variables: The bit energy  $E_b$  and the channel coefficient  $\lambda$ .

#### A. BER computation methodology under AWGN channel

In this section, the AWGN channel is considered to highlight the non constant bit energy problem. In this case, the channel coefficient is constant equal to one  $\lambda = 1$  and  $\gamma_b = E_b / N_0$ . In order to compute (28), it is necessary to get the bit energy distribution for a given chaotic map and a spreading factor.

For this aim, we fitted the histogram of the energy distribution for the CPF sequence. Figure 5 shows the histogram of the bit energy after spreading by the CPF chaotic sequence for  $\beta = 20$ . This histogram has been obtained using ten million samples. From these samples, energies of successive bits are calculated for a given spreading factor. The bit energy is assumed to be the output of a stationary random process [36]; hence the histogram obtained in Figure 5 can be considered

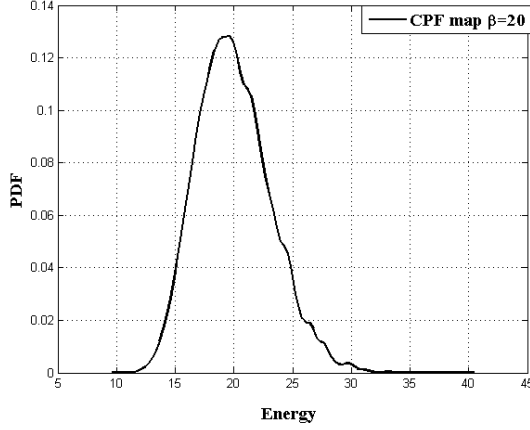


Fig. 5. Histogram of the bit energy distribution  $E_b$  for  $\beta = 20$

as a good estimation of the probability density function of the bit energy.

Given the shape of this energy distribution, the analytical expression appears difficult to compute, leaving numerical integration as a solution for performing the BER computation. The expression (28) can be computed numerically, taking into account the bit-energy variation.

#### BER computation methodology under Rayleigh channel

The objective is to compute the BER given in equation (28) by taking into account both the bit energy and the channel coefficient. The analytical derivation of  $\gamma_b$  seems difficult because the bit energy have an irregular PDF shape. An alternative solution consists to estimate the PDF of  $\gamma_b$ , then integrated equation (28) numerically.

### VI. SIMULATION RESULTS AND DISCUSSIONS

To evaluate the effect of the number of subcarriers on performance, we plot the computed BER expressions with simulation results of the MC-DCSK system over an AWGN and Rayleigh channels. The results obtained are for different numbers of subcarriers  $M$  and spreading factors  $\beta$ .

The parameters of the simulation in a mono-user case are set as follows: the MC-DCSK system uses the square-root-raised-cosine chip waveform for a roll-off factor  $\alpha$  equal to 0.25. As shown in equation (6), the spreading factor is computed as a function of the number of subcarriers  $M$ , the bit duration  $T_b$ , and the total allocated bandwidth  $B$ . In our simulations, we set the bit duration  $T_b = 400$ ,  $B = 1$  and for  $M = 64$  the allowed spreading factor  $\beta = 5$ , for  $M = 16$  subcarriers  $\beta = 20$ , for  $M = 8$   $\beta = 40$ , and for  $M = 2$   $\beta = 160$ .

Figure 6 presents the performances obtained from the BER expression of (28) and the Monte Carlo simulations of the MC-DCSK system under AWGN channel. It clearly appears that there are an excellent match between simulations and our computed BER expression for any number of subcarrier and spreading factor.

In Figure 7 we study the effect of the number of subcarriers on the system performance under AWGN channel. To that end,

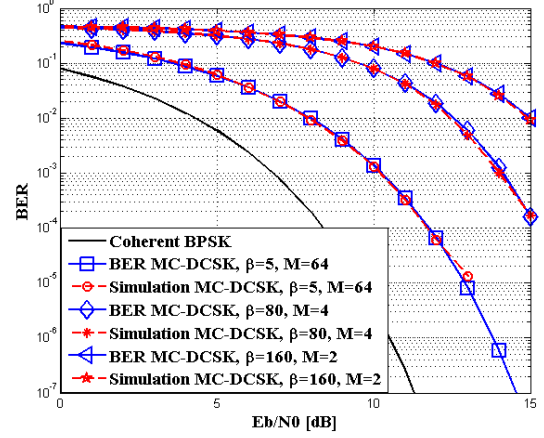


Fig. 6. Simulation and BER expression, for different values of spreading factor  $\beta$ , number of subcarrier  $M$ , and under AWGN channel

we set the spreading factor to  $\beta = 5$  and the bit duration  $T_b$ , and then we assume that the bandwidth  $B$  is wide enough to support any number of subcarriers  $M$ . Figure 7 shows interesting results of our proposed MC-DCSK system in terms of performance enhancement. In fact, for a given spreading factor, when the number of subcarriers  $M$  increases, the  $DBR$  ratio tends toward one, meaning that less reference energy used to transmit one bit or the reference energy is shared with more  $M - 1$  bit. This performance improvement proven in expression (28) means that for high number of subcarriers  $M$ , we need less energy to reach a given BER. In this figure, we show the performance improvement by simulation for  $M = 2$  and  $M = 64$ , with a fixed spreading factor equal to  $\beta = 5$ . In the case of  $M = 2$ , the MC-DCSK system is equivalent to a DCSK system. The result shown in Figure 7 can be seen as a performance comparison between the proposed system with that of the conventional DCSK.

In the same Figure, we can observe a degradation in performance between the MC-DCSK system for  $M = 64$  and the coherent BPSK one. This degradation comes from the two noise sources added to the reference and the data carrier signals.

To understand the performance behavior of MC-DCSK system for different spreading factor the optimal spreading factor must be discussed. The optimal spreading factor was studied in [37] for single carrier DCSK system. Figure 8 evaluates the effect of the value of the spreading factor on the performance of the MC-DCSK under AWGN channel. The simulated bit error rate is plotted for different values of spreading factor  $\beta$  with a fixed  $E_b/N_0$  and number of subcarriers  $M = 2$ . The bandwidth is assumed to be wide enough to support any spreading factor value. Because the BER expression is approximated and computed by numerical integration, the theory in this case can only qualitatively describe the dependence of the MC-DCSK of spreading factor. Simulation shows that the intermediate spreading factor values between 5 and 50 minimize bit error rates at fixed  $E_b/N_0$ . From this result, we see that good performances are obtained for low spreading factor values which makes this system

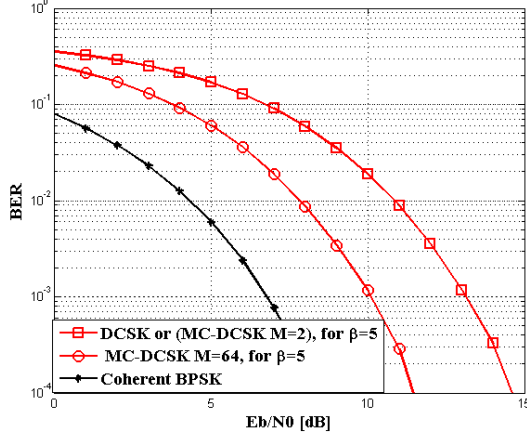


Fig. 7. BER comparison of MC-DCSK for  $M=64$  and DCSK (i.e MC-DCSK for  $M=2$ ) where the spreading factor  $\beta = 5$  under AWGN channel

implementation feasible even for moderate bandwidth.

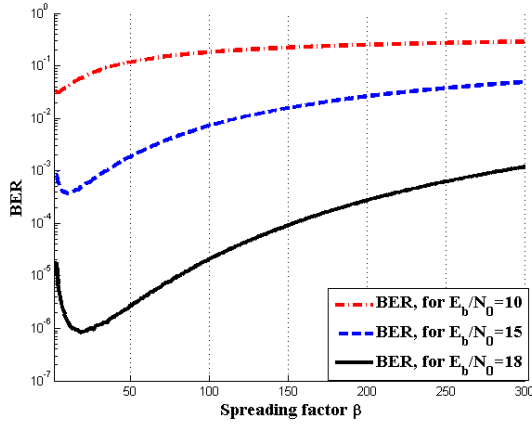


Fig. 8. BER versus the spreading sequence length for MC-DCSK for  $M=2$

Figures 9, and 10, evaluate the effect of the Rayleigh channel on the performance of the MC-DCSK system. The computed bit error rate given in equation (28) and the computer simulation of the BER are performed. The system's performance plotted in Figure 9 is evaluated for two different subcarriers  $M = 2$  and  $M = 64$ , spreading factor equal to  $\beta = 5$ , and an average gain power of the channel  $E(\lambda^2) = 0.7$ .

In Figure 10, the performance is evaluated for two different subcarriers  $M = 2$  and  $M = 64$ , spreading factor equal to  $\beta = 50$ , and an average gain power of the channel  $E(\lambda^2) = 0.9$ .

It clearly appears that there are an excellent match between simulations and our computed BER expression for any number of subcarrier, average gain power, and spreading factor.

#### Discussions

The proposed system meets the following properties:

- Non-coherent system: Robust receiver;
- Spread spectrum system: resistance to interferences;

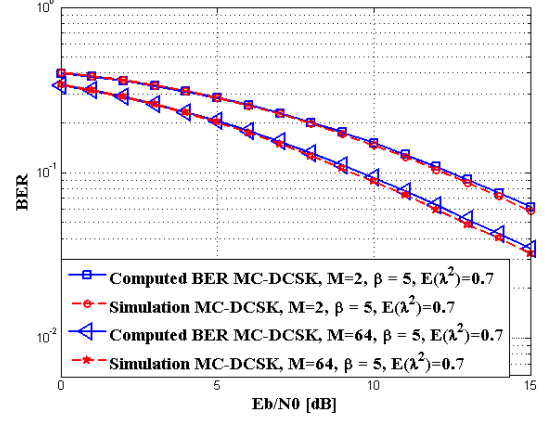


Fig. 9. Simulation and BER expression, for a spreading factor  $\beta = 5$ , number of subcarrier  $M = 2$   $M = 64$  under Rayleigh channel with average gain power  $E(\lambda^2) = 0.7$

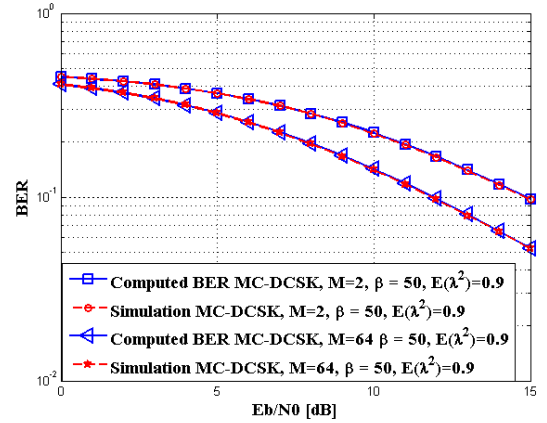


Fig. 10. Simulation and BER expression, for a spreading factor  $\beta = 50$ , number of subcarrier  $M = 2$   $M = 64$  under Rayleigh channel with average gain power  $E(\lambda^2) = 0.9$

- Chaotic signals: easy to generate, low PAPR in multi-carrier transmissions, good correlation properties;
- Multi-carrier DCSK: high spectral efficiency, low power consumption.

#### VII. CONCLUSION

An energy-efficient non-coherent multi-carrier spread spectrum system has been presented. From the outstanding energy inefficiency drawback imposed by time-multiplexed differential modulations, a novel frequency multiplexed architecture is designed. The multi-carrier characteristic of this novel design enables significant energy savings and a higher spectral efficiency as compared to differential systems because in the new system, the reference signal is only sent once for many parallel bits. The energy efficiency of the proposed system is analyzed and a *DBR* is derived, with results showing that for  $M > 20$  subcarriers, the energy lost in transmitting the reference is less than 5% of the total bit energy per bit. The performance of the proposed system is studied, the bit error rate expression is derived for Rayleigh fading channels, and



simulation results match the theoretical expression, proving the accuracy of our approach. To compare the performance of the proposed system with that of the DCSK, the simulated BERs are plotted with the same spreading factor, where results prove an increase in performance as compared to the conventional DCSK. Our future work will focus on defining multi-user access strategies and performance improvement of this system.

## REFERENCES

- [1] K. David, D. Dixit, and N. Jefferies, "2020 Vision," *IEEE Vehicular Technology Mag.*, vol. 5, no. 3, pp. 22–29, Sept. 2010.
- [2] J. de Mingo, A. Valdovinos, A. Crespo, D. Navarro, and P. Garcia, "An RF electronically controlled impedance tuning network design and its application to an antenna input impedance automatic matching system," *IEEE Trans. Microwave Theory and Tech.*, vol. 52, no. 2, pp. 489–497, Feb. 2004.
- [3] J. Karedal, F. Tufvesson, N. Czink, A. Paier, C. Dumard, T. Zemen, C. Mecklenbrauker, and A. Molisch, "A geometry-based stochastic MIMO model for vehicle-to-vehicle communications," *IEEE Trans. Wireless Commun.*, vol. 8, no. 7, pp. 3646–3657, July 2009.
- [4] B. Le Saux, M. Helard, and P.-J. Bouvet, "Comparison of coherent and non-coherent space time schemes for frequency selective fast-varying channels," in *Proc. 2005 International Symposium on Wireless Communication Systems (ISWCS)*, pp. 32–36.
- [5] L. Hanzo, T. Keller, M. Muenster, and B.-J. Choi, *OFDM and MC-CDMA for Broadband Multi-User Communications, WLANs and Broadcasting*. New York, NY, USA: John Wiley & Sons, Inc., 2003.
- [6] R. V. Nee and R. Prasad, *OFDM for Wireless Multimedia Communications*, 1st ed. Norwood, MA, USA: Artech House, Inc., 2000.
- [7] S. Kondo and B. Milstein, "Performance of multicarrier DS-CDMA systems," *IEEE Trans. Commun.*, vol. 44, no. 2, pp. 238–246, Feb 1996.
- [8] F. C. M. Lau and C. K. Tse, *Chaos-Based Digital communication systems*. Springer-Verlag, 2003.
- [9] A. P. Kurian, S. Puthusserypady, and S. M. Htut, "Performance enhancement of DS-CDMA system using chaotic complex spreading sequence," *IEEE Trans. Wireless Commun.*, vol. 4, no. 3, pp. 984–989, May 2005.
- [10] R. Vali, S. Berber, and S. K. Nguang, "Accurate derivation of chaos-based acquisition performance in a fading channel," *IEEE Trans. Wireless Commun.*, vol. 11, no. 2, pp. 722–731, february 2012.
- [11] J. Yu and Y.-D. Yao, "Detection performance of chaotic spreading LPI waveforms," *IEEE Trans. Wireless Commun.*, vol. 4, no. 2, pp. 390–396, march 2005.
- [12] V. Lynnyk and S. Celikovskiy, "On the anti-synchronization detection for the generalized lorenz system and its application to secure encryption," *Kybernetika*, vol. 46, pp. 1–18, 2010.
- [13] S. Vitali, R. Rovatti, and G. Setti, "Improving PA efficiency by chaos-based spreading in multicarrier DS-CDMA systems," in *Proc. 2006 IEEE International Symposium on Circuits and Systems (ISCAS)*, May 2006, pp. 4 pp. –1198.
- [14] G. Kolumbán, G. Kis, Z. Jákó, and M. P. Kennedy, "FM-DCSK: A robust modulation scheme for chaotic communications," *IEICE Trans. Fundamentals of Electronics, Communications and Computer*, vol. 89, pp. 1798–1802, 1998.
- [15] Y. Xia, C. K. Tse, and F. C. M. Lau, "Performance of differential chaos-shift-keying digital communication systems over a multipath fading channel with delay spread," *IEEE Trans. Circuits and Systems II*, vol. 51, pp. 680–684, 2004.
- [16] G. Kaddoum, F. Gagnon, P. Charge, and D. Roviras, "A generalized ber prediction method for differential chaos shift keying system through different communication channels," *Wireless Personal Communications*, vol. 64, pp. 425–437, 2012.
- [17] Y. Fang, L. W. J. Xu, and G. Chen, "Performance of MIMO relay DCSK-CD systems over nakagami fading channels," *IEEE Trans. on Circuits and systems I*, vol. 60, pp. 1–11, March 2013.
- [18] Y. Fang, L. Wang, and G. Chen, "Performance of a multiple-access DCSK-CC system over nakagami-m fading channels," in *Proc. 2013 IEEE International Symposium on Circuits and Systems (ISCAS)*, 2013.
- [19] W. Xu, L. Wang, and G. Chen, "Performance of DCSK cooperative communication systems over multipath fading channels," *IEEE Trans. on Circuits and Systems I: Regular Papers*, vol. 58, no. 1, pp. 196–204, jan. 2011.
- [20] J. Xu, W. Xu, L. Wang, and G. Chen, "Design and simulation of a cooperative communication system based on DCSK/FM-DCSK," in *Proc. 2010 IEEE International Symposium on Circuits and Systems (ISCAS)*, 30 2010-june 2 2010, pp. 2454–2457.
- [21] G. Kaddoum, F. Gagnon, and F.-D. Richardson, "Design of a secure Multi-Carrier DCSK system," in *Proc. 2012 The ninth international symposium on wireless communication systems ( ISWCS )*, June 2012, pp. 964–968.
- [22] H. Yang and G.-P. Jiang, "High-efficiency differential-chaos-shift-keying scheme for chaos-based noncoherent communication," *IEEE Trans. Circuits and Systems-II*, vol. 59, no. 5, pp. 312–316, May 2012.
- [23] W. K. Xu, L. Wang, and K. G., "A novel differential chaos shift keying modulation scheme," *Trans. International Journal of Bifurcation and Chaos*, vol. 21, no. 03, pp. 799–814, 2011.
- [24] G. Kaddoum and F. Gagnon, "Design of a high-data-rate differential chaos-shift keying system," *IEEE Trans. on Circuits and Systems-II*, vol. 59, no. 99, pp. 1–5, July 2012.
- [25] G. Cimatti, R. Rovatti, and G. Setti, "Chaos-based spreading in DS-UWB sensor networks increases available bit rate," *IEEE Trans. on Circuits and Systems I: Regular Papers*, vol. 54, no. 6, pp. 1327–1339, june 2007.
- [26] C.-C. Chong and S. K. Yong, "UWB direct chaotic communication technology for low-rate WPAN applications," *IEEE Trans. Vehicular Technology*, vol. 57, no. 3, pp. 1527–1536, May 2008.
- [27] X. Min, W. Xu, L. Wang, and G. Chen, "Promising performance of a frequency-modulated differential chaos shift keying ultra-wideband system under indoor environments," *IET Trans. on Communications*, vol. 4, no. 2, pp. 125–134, 22 2010.
- [28] Z. Zhibo, Z. Tong, and W. Jinxiang, "Performance of multiple-access DCSK communication over a multipath fading channel with delay spread," *Circuits, Systems and Signal Processing*, vol. 27, pp. 507–518, 2008.
- [29] A. J. Lawrance and G. Ohama, "Exact calculation of bit error rates in communication systems with chaotic modulation," *IEEE Trans. Circuits and Systems-I*, vol. 50, pp. 1391–1400, November 2003.
- [30] J. Yao and A. J. Lawrance, "Performance analysis and optimization of multi-user differential chaos-shift keying communication systems," *IEEE Trans. Circuits and Systems-I*, vol. 53, pp. 2075–2091, September 2006.
- [31] Z. Zhibo, W. Jinxiang, and Y. Yizheng, "Exact BER analysis of differential chaos shift keying communication system in fading channels," *Springer Wirel. Pers. Commun.*, vol. 53, no. 2, pp. 299–310, 2010.
- [32] A. Nayak and I. Stojmenovic, *Wireless Sensor and Actuator Networks: Algorithms and Protocols for Scalable Coordination and Data Communication*, 1st ed. Wiley-IEEE Press, 2010.
- [33] G. Kaddoum, P. Chargé, D. Roviras, and D. Fournier-Prunaret, "A methodology for bit error rate prediction in chaos-based communication systems," *Birkhäuser, Circuits, Systems and Signal Processing*, vol. 28, pp. 925–944, 2009.
- [34] M. Sushchik, L. S. Tsimring, and A. R. Volkovskii, "Performance analysis of correlation-based communication schemes utilizing chaos," *IEEE Trans. Circuits and Systems I*, vol. 47, pp. 1684–1691, 2000.
- [35] G. Kaddoum, P. Chargé, and D. Roviras, "A generalized methodology for bit-error-rate prediction in correlation-based communication schemes using chaos," *IEEE Commun. Letters*, vol. 13, no. 8, pp. 567–569, 2009.
- [36] S. H. Isabelle and G. W. Wornell, "Statistical analysis and spectral estimation techniques for one-dimensional chaotic signals," *IEEE Trans. Signal Processing*, vol. 45, pp. 1495–1497, 1997.
- [37] J. Yao and A. Lawrance, "Optimal spreading in multi-user non-coherent binary chaos-shift-keying communication systems," in *Proc. 2005 IEEE International Symposium on Circuits and Systems (ISCAS)*, vol. 2, may 2005, pp. 876–879.